Research Article | Vol. 9, No. 9 | 1 Sep 2018 | BIOMEDICAL OPTICS EXPRESS 4149
Biomedical Optics EXPRESS

Label-free real-time ultrasensitive monitoring of non-small cell lung cancer cell interaction with drugs

HAILANG DAI,[1,2] YIHANG JIAO,[1,2] ZHANGCHI SUN,[3] ZHUANGQI CAO,[1] AND XIANFENG CHEN[1,2,*]

[1]*The State Key Laboratory on Fiber Optic Local Area Communication Networks and Advanced Optical Communication Systems, School of Physics and Astronomy, Shanghai JiaoTong University, Shanghai 200240, China*
[2]*Collaborative Innovation Center of IFSA (CICIFSA), Shanghai Jiao Tong University, Shanghai 200240, China*
[3]*Zhejiang Rongjun Hospital, Jiaxing 314000, China*
**xfchen@sjtu.edu.cn*

Abstract: The timely discovery of cancer cell resistance in clinical processing and the accurate calculation of drug dosage to reduce and inhibit tumour growth factor in cancer patients are promising technologies in cancer therapy. Here, an optofluidic resonator effectively detects drug interactions with cancer cell processing in real time and enables the calculation of label-free drug-non-small cell lung cancer (NSCLC) epidermal growth factor receptor (EGFR) and binding ratios using molecular fluorescence intensity. According to clinical test and in vivo experimental data, the efficiencies of gefitinib and erlotinib are only 37% and 12% compared to AZD9291, and 0.300 μg of EGFR inactivation requires 0.484 μg of AZD9291, 0.815 μg of gefitinib and 1.348 μg of erlotinib. Experimental results show that the present method allows for the performance detection of drug resistance and for the evaluation of dosage usage.

OCIS codes: (170.0170) Medical optics and biotechnology; (170.4580) Optical diagnostics for medicine; (170.6930) Tissue; (140.4780) Optical resonators; (140.0140) Lasers and laser optics.

References and links

1. A. J. Barker, K. H. Gibson, W. Grundy, A. A. Godfrey, J. J. Barlow, M. P. Healy, J. R. Woodburn, S. E. Ashton, B. J. Curry, L. Scarlett, L. Henthorn, and L. Richards, "Studies leading to the identification of ZD1839 (IRESSA): an orally active, selective epidermal growth factor receptor tyrosine kinase inhibitor targeted to the treatment of cancer," Bioorg. Med. Chem. Lett. **11**(14), 1911–1914 (2001).
2. J. D. Moyer, E. G. Barbacci, K. K. Iwata, L. Arnold, B. Boman, A. Cunningham, C. DiOrio, J. Doty, M. J. Morin, M. P. Moyer, M. Neveu, V. A. Pollack, L. R. Pustilnik, M. M. Reynolds, D. Sloan, A. Theleman, and P. Miller, "Induction of apoptosis and cell cycle arrest by CP-358,774, an inhibitor of epidermal growth factor receptor tyrosine kinase," Cancer Res. **57**(21), 4838–4848 (1997).
3. T. J. Lynch, D. W. Bell, R. Sordella, S. Gurubhagavatula, R. A. Okimoto, B. W. Brannigan, P. L. Harris, S. M. Haserlat, J. G. Supko, F. G. Haluska, D. N. Louis, D. C. Christiani, J. Settleman, and D. A. Haber, "Activating mutations in the epidermal growth factor receptor underlying responsiveness of non-small-cell lung cancer to gefitinib," N. Engl. J. Med. **350**(21), 2129–2139 (2004).
4. J. Guillermo Paez and P. Pasi Janne, J. C. Lee, S. Tracy, H. Greulich, S. Gabriel, P. Herman, F. J. Kaye, N. Lindeman, T. J. Boggon, K. Naoki, H. Sasaki, Y. Fujii, M. J. Eck, W. R. Sellers, B. E. Johnson, M. Meyerson, "EGFR mutations in lung cancer: correlation with clinical response to geftinib therapy," Science **304**, 1497–1500 (2004).
5. W. Pao, V. Miller, M. Zakowski, J. Doherty, K. Politi, I. Sarkaria, B. Singh, R. Heelan, V. Rusch, L. Fulton, E. Mardis, D. Kupfer, R. Wilson, M. Kris, and H. Varmus, "EGF receptor gene mutations are common in lung cancers from "never smokers" and are associated with sensitivity of tumors to gefitinib and erlotinib," Proc. Natl. Acad. Sci. U.S.A. **101**(36), 13306–13311 (2004).
6. W. Pao and J. Chmielecki, "Rational, biologically based treatment of EGFR-mutant non-small-cell lung cancer," Nat. Rev. Cancer **10**(11), 760–774 (2010).
7. M. Maemondo, A. Inoue, K. Kobayashi, S. Sugawara, S. Oizumi, H. Isobe, A. Gemma, M. Harada, H. Yoshizawa, I. Kinoshita, Y. Fujita, S. Okinaga, H. Hirano, K. Yoshimori, T. Harada, T. Ogura, M. Ando, H.

#335693 https://doi.org/10.1364/BOE.9.004149
Journal © 2018 Received 20 Jun 2018; revised 19 Jul 2018; accepted 1 Aug 2018; published 7 Aug 2018

Biomedical Optics EXPRESS

Miyazawa, M. S. T. Tanaka, Y. Saijo, K. Hagiwara, S. Morita, and T. Nukiwa, "Geftinib or chemotherapy for non-small-cell lung cancer with mutated EGFR," N. Engl. J. Med. **362**, 2380–2388 (2010).
8. T. Mitsudomi, S. Morita, Y. Yatabe, S. Negoro, I. Okamoto, J. Tsurutani, T. Seto, M. Satouchi, H. Tada, T. Hirashima, K. Asami, N. Katakami, M. Takada, H. Yoshioka, K. Shibata, S. Kudoh, E. Shimizu, H. Saito, S. Toyooka, K. Nakagawa, and M. Fukuoka, "Gefitinib versus cisplatin plus docetaxel in patients with non-small-cell lung cancer harbouring mutations of the epidermal growth factor receptor (WJTOG3405): an open label, randomised phase 3 trial," Lancet Oncol. **11**(2), 121–128 (2010).
9. T. S. Mok, Y. L. Wu, S. Thongprasert, C. H. Yang, D. T. Chu, N. Saijo, P. Sunpaweravong, B. Han, B. Margono, Y. Ichinose, Y. Nishiwaki, Y. Ohe, J. J. Yang, B. Chewaskulyong, H. Jiang, E. L. Duffield, C. L. Watkins, A. A. Armour, and M. Fukuoka, "Gefitinib or carboplatin-paclitaxel in pulmonary adenocarcinoma," N. Engl. J. Med. **361**(10), 947–957 (2009).
10. R. Rosell, E. Carcereny, R. Gervais, A. Vergnenegre, B. Massuti, E. Felip, R. Palmero, R. Garcia-Gomez, C. Pallares, J. M. Sanchez, R. Porta, M. Cobo, P. Garrido, F. Longo, T. Moran, A. Insa, F. De Marinis, R. Corre, I. Bover, A. Illiano, E. Dansin, J. de Castro, M. Milella, N. Reguart, G. Altavilla, U. Jimenez, M. Provencio, M. A. Moreno, J. Terrasa, J. Muñoz-Langa, J. Valdivia, D. Isla, M. Domine, O. Molinier, J. Mazieres, N. Baize, R. Garcia-Campelo, G. Robinet, D. Rodriguez-Abreu, G. Lopez-Vivanco, V. Gebbia, L. Ferrera-Delgado, P. Bombaron, R. Bernabe, A. Bearz, A. Artal, E. Cortesi, C. Rolfo, M. Sanchez-Ronco, A. Drozdowskyj, C. Queralt, I. de Aguirre, J. L. Ramirez, J. J. Sanchez, M. A. Molina, M. Taron, and L. Paz-Ares, "Erlotinib versus standard chemotherapy as first-line treatment for European patients with advanced EGFR mutation-positive non-small-cell lung cancer (EURTAC): a multicentre, open-label, randomised phase 3 trial," Lancet Oncol. **13**(3), 239–246 (2012).
11. C. Zhou, Y. L. Wu, G. Chen, J. Feng, X. Q. Liu, C. Wang, S. Zhang, J. Wang, S. Zhou, S. Ren, S. Lu, L. Zhang, C. Hu, C. Hu, Y. Luo, L. Chen, M. Ye, J. Huang, X. Zhi, Y. Zhang, Q. Xiu, J. Ma, L. Zhang, and C. You, "Erlotinib versus chemotherapy as first-line treatment for patients with advanced EGFR mutation-positive non-small-cell lung cancer (OPTIMAL, CTONG-0802): a multicentre, open-label, randomised, phase 3 study," Lancet Oncol. **12**(8), 735–742 (2011).
12. B. Burtness, M. Anadkat, S. Basti, M. Hughes, M. E. Lacouture, J. S. McClure, P. L. Myskowski, J. Paul, C. S. Perlis, L. Saltz, and S. Spencer, "NCCN Task Force Report: Management of dermatologic and other toxicities associated with EGFR inhibition in patients with cancer," J. Natl. Compr. Canc. Netw. **7**(1), S5–S21, quiz S22–S24 (2009).
13. K. Takezawa, V. Pirazzoli, M. E. Arcila, C. A. Nebhan, X. Song, E. de Stanchina, K. Ohashi, Y. Y. Janjigian, P. J. Spitzler, M. A. Melnick, G. J. Riely, M. G. Kris, V. A. Miller, M. Ladanyi, K. Politi, and W. Pao, "HER2 amplification: a potential mechanism of acquired resistance to EGFR inhibition in EGFR-mutant lung cancers that lack the second-site EGFRT790M mutation," Cancer Discov. **2**(10), 922–933 (2012).
14. J. Bean, C. Brennan, J. Y. Shih, G. Riely, A. Viale, L. Wang, D. Chitale, N. Motoi, J. Szoke, S. Broderick, M. Balak, W. C. Chang, C. J. Yu, A. Gazdar, H. Pass, V. Rusch, W. Gerald, S. F. Huang, P. C. Yang, V. Miller, M. Ladanyi, C. H. Yang, and W. Pao, "MET amplification occurs with or without T790M mutations in EGFR mutant lung tumors with acquired resistance to gefitinib or erlotinib," Proc. Natl. Acad. Sci. U.S.A. **104**(52), 20932–20937 (2007).
15. J. A. Engelman, K. Zejnullahu, T. Mitsudomi, Y. Song, C. Hyland, J. O. Park, N. Lindeman, C. M. Gale, X. Zhao, J. Christensen, T. Kosaka, A. J. Holmes, A. M. Rogers, F. Cappuzzo, T. Mok, C. Lee, B. E. Johnson, L. C. Cantley, and P. A. Jänne, "MET amplification leads to gefitinib resistance in lung cancer by activating ERBB3 signaling," Science **316**(5827), 1039–1043 (2007).
16. L. V. Sequist, B. A. Waltman, D. Dias-Santagata, S. Digumarthy, A. B. Turke, P. Fidias, K. Bergethon, A. T. Shaw, S. Gettinger, A. K. Cosper, S. Akhavanfard, R. S. Heist, J. Temel, J. G. Christensen, J. C. Wain, T. J. Lynch, K. Vernovsky, E. J. Mark, M. Lanuti, A. J. Iafrate, M. Mino-Kenudson, and J. A. Engelman, "Genotypic and histological evolution of lung cancers acquiring resistance to EGFR inhibitors," Sci. Transl. Med. **3**(75), 75ra26 (2011).
17. K. Ohashi, L. V. Sequist, M. E. Arcila, T. Moran, J. Chmielecki, Y. L. Lin, Y. Pan, L. Wang, E. de Stanchina, K. Shien, K. Aoe, S. Toyooka, K. Kiura, L. Fernandez-Cuesta, P. Fidias, J. C. Yang, V. A. Miller, G. J. Riely, M. G. Kris, J. A. Engelman, C. L. Vnencak-Jones, D. Dias-Santagata, M. Ladanyi, and W. Pao, "Lung cancers with acquired resistance to EGFR inhibitors occasionally harbor BRAF gene mutations but lack mutations in KRAS, NRAS, or MEK1," Proc. Natl. Acad. Sci. U.S.A. **109**(31), E2127–E2133 (2012).
18. E. C. de Bruin, C. Cowell, P. H. Warne, M. Jiang, R. E. Saunders, M. A. Melnick, S. Gettinger, Z. Walther, A. Wurtz, G. J. Heynen, D. A. Heideman, J. Gómez-Román, A. García-Castaño, Y. Gong, M. Ladanyi, H. Varmus, R. Bernards, E. F. Smit, K. Politi, and J. Downward, "Reduced NF1 expression confers resistance to EGFR inhibition in lung cancer," Cancer Discov. **4**(5), 606–619 (2014).
19. K. E. Ware, M. E. Marshall, L. R. Heasley, L. Marek, T. K. Hinz, P. Hercule, B. A. Helfrich, R. C. Doebele, and L. E. Heasley, "Rapidly acquired resistance to EGFR tyrosine kinase inhibitors in NSCLC cell lines through de-repression of FGFR2 and FGFR3 expression," PLoS One **5**(11), e14117 (2010).
20. S. Kobayashi, T. J. Boggon, T. Dayaram, P. A. Jänne, O. Kocher, M. Meyerson, B. E. Johnson, M. J. Eck, D. G. Tenen, and B. Halmos, "EGFR mutation and resistance of non-small-cell lung cancer to gefitinib," N. Engl. J. Med. **352**(8), 786–792 (2005).

Biomedical Optics EXPRESS

21. W. Pao, V. A. Miller, K. A. Politi, G. J. Riely, R. Somwar, M. F. Zakowski, M. G. Kris, and H. Varmus, "Acquired resistance of lung adenocarcinomas to gefitinib or erlotinib is associated with a second mutation in the EGFR kinase domain," PLoS Med. **2**(3), e73 (2005).
22. M. L. Sos, H. B. Rode, S. Heynck, M. Peifer, F. Fischer, S. Klüter, V. G. Pawar, C. Reuter, J. M. Heuckmann, J. Weiss, L. Ruddigkeit, M. Rabiller, M. Koker, J. R. Simard, M. Getlik, Y. Yuza, T. H. Chen, H. Greulich, R. K. Thomas, and D. Rauh, "Chemogenomic profiling provides insights into the limited activity of irreversible EGFR Inhibitors in tumor cells expressing the T790M EGFR resistance mutation," Cancer Res. **70**(3), 868–874 (2010).
23. C. H. Yun, K. E. Mengwasser, A. V. Toms, M. S. Woo, H. Greulich, K. K. Wong, M. Meyerson, and M. J. Eck, "The T790M mutation in EGFR kinase causes drug resistance by increasing the affinity for ATP," Proc. Natl. Acad. Sci. U.S.A. **105**(6), 2070–2075 (2008).
24. D. Li, L. Ambrogio, T. Shimamura, S. Kubo, M. Takahashi, L. R. Chirieac, R. F. Padera, G. I. Shapiro, A. Baum, F. Himmelsbach, W. J. Rettig, M. Meyerson, F. Solca, H. Greulich, and K. K. Wong, "BIBW2992, an irreversible EGFR/HER2 inhibitor highly effective in preclinical lung cancer models," Oncogene **27**(34), 4702–4711 (2008).
25. J. A. Engelman, K. Zejnullahu, C. M. Gale, E. Lifshits, A. J. Gonzales, T. Shimamura, F. Zhao, P. W. Vincent, G. N. Naumov, J. E. Bradner, I. W. Althaus, L. Gandhi, G. I. Shapiro, J. M. Nelson, J. V. Heymach, M. Meyerson, K. K. Wong, and P. A. Jänne, "PF00299804, an irreversible pan-ERBB inhibitor, is effective in lung cancer models with EGFR and ERBB2 mutations that are resistant to gefitinib," Cancer Res. **67**(24), 11924–11932 (2007).
26. S. S. Ramalingam, F. Blackhall, M. Krzakowski, C. H. Barrios, K. Park, I. Bover, D. Seog Heo, R. Rosell, D. C. Talbot, R. Frank, S. P. Letrent, A. Ruiz-Garcia, I. Taylor, J. Q. Liang, A. K. Campbell, J. O'Connell, and M. Boyer, "Randomized phase II study of dacomitinib (PF-00299804), an irreversible pan-human epidermal growth factor receptor inhibitor, versus erlotinib in patients with advanced non-small-cell lung cancer," J. Clin. Oncol. **30**(27), 3337–3344 (2012).
27. Y. Sako, S. Minoghchi, and T. Yanagida, "Single-molecule imaging of EGFR signalling on the surface of living cells," Nat. Cell Biol. **2**(3), 168–172 (2000).
28. J. Homola, "Surface plasmon resonance sensors for detection of chemical and biological species," Chem. Rev. **108**(2), 462–493 (2008).
29. M. J. Garnett, E. J. Edelman, S. J. Heidorn, C. D. Greenman, A. Dastur, K. W. Lau, P. Greninger, I. R. Thompson, X. Luo, J. Soares, Q. Liu, F. Iorio, D. Surdez, L. Chen, R. J. Milano, G. R. Bignell, A. T. Tam, H. Davies, J. A. Stevenson, S. Barthorpe, S. R. Lutz, F. Kogera, K. Lawrence, A. McLaren-Douglas, X. Mitropoulos, T. Mironenko, H. Thi, L. Richardson, W. Zhou, F. Jewitt, T. Zhang, P. O'Brien, J. L. Boisvert, S. Price, W. Hur, W. Yang, X. Deng, A. Butler, H. G. Choi, J. W. Chang, J. Baselga, I. Stamenkovic, J. A. Engelman, S. V. Sharma, O. Delattre, J. Saez-Rodriguez, N. S. Gray, J. Settleman, P. A. Futreal, D. A. Haber, M. R. Stratton, S. Ramaswamy, U. McDermott, and C. H. Benes, "Systematic identification of genomic markers of drug sensitivity in cancer cells," Nature **483**(7391), 570–575 (2012).
30. K. Heinzmann, L. M. Carter, J. S. Lewis, and E. O. Absagye, "Multiplexed imaging for diagnosis and therapy," Nature Biomedical Engineering **1**(9), 697–713 (2017).
31. P. Andrew and W. L. Barnes, "Energy transfer across a metal film mediated by surface plasmon polaritons," Science **306**(5698), 1002–1005 (2004).
32. X. Fan and I. M. White, "Optofluidic microsystems for chemical and biological analysis," Nat. Photonics **5**(10), 591–597 (2011).
33. Y. Wang, Z. Cao, T. Yu, H. Li, and Q. Shen, "Enhancement of the superprism effect based on the strong dispersion effect of ultrahigh-order modes," Opt. Lett. **33**(11), 1276–1278 (2008).
34. X. Fan, I. M. White, S. I. Shopova, H. Zhu, J. D. Suter, and Y. Sun, "Sensitive optical biosensors for unlabeled targets: a review," Anal. Chim. Acta **620**(1-2), 8–26 (2008).
35. H. Dai, Z. Cao, Y. Wang, H. Li, M. Sang, W. Yuan, F. Chen, and X. Chen, "Concentric circular grating generated by the patterning trapping of nanoparticles in an optofluidic chip," Sci. Rep. **6**(1), 32018–32025 (2016).
36. Y. Zheng, Z. Cao, and X. Chen, "Conical reflection of light during free-space coupling into a symmetrical metal-cladding waveguide," J. Opt. Soc. Am. A **30**(9), 1901–1904 (2013).
37. C. H. Yun, T. J. Boggon, Y. Li, M. S. Woo, H. Greulich, M. Meyerson, and M. J. Eck, "Structures of lung cancer-derived EGFR mutants and inhibitor complexes: mechanism of activation and insights into differential inhibitor sensitivity," Cancer Cell **11**(3), 217–227 (2007).
38. W. Yuan, C. Yin, H. Li, P. Xiao, and Z. Cao, "Wideband slow light assisted by ultrahigh-order modes," J.O.S.A.B **28**(5), 968–971 (2011).
39. R. Horvath, H. C. Pedersen, and N. B. Larsen, "Demonstration of reverse symmetry waveguide sensing in aqueous solutions," Appl. Phys. Lett. **81**(12), 2166–2168 (2002).

1. Introduction

Erlotinib and gefitinib tyrosine kinase inhibitors (TKIs) were serendipitously found to be the most effective in advanced NSCLC clinical development [1]. They are reversible small-molecule ATP analogues originally designed to inhibit the TK activity of wild-type EGFR [2]. However, patients ultimately develop disease progression, often driven by the acquisition

Biomedical Optics EXPRESS

of a second T790M EGFR TKI resistance mutation [3]. AZD9291 is a novel oral, potent, and selective third-generation irreversible inhibitor of both EGFR-mutant sensitizing and T790M resistance mutants that spares wild-type EGFR [4, 5]. Unfortunately, although patients with EGFR-mutant tumours typically show a good initial response to TKIs, most tumour-tissue patients have a number of mechanisms that mediate EGFR TKI resistance [6–10] after approximately 9 to 14 months of continuous treatment [11–15]. Furthermore, these TKIs are associated with side effects that include skin rash and diarrhoea that are due to inhibition of wild-type EGFR in skin and gastrointestinal organs [16]. In the clinic, the keys of factors of chemotherapy failure are resistance and side effects. As a monotherapy, they have failed to overcome EGFR-mutant mediated resistance in patients, and it is difficult to control the quantity of drugs for inhibition of wild-type EGFR or cell injury in cancer therapy [17, 18].

Recently, preclinical modeling and analysis of tumor tissue obtained from patients in the study of the disease have been employed. Such genetic technology [19–25] has led to the identification of a number of mechanisms that mediate EGFR TKI resistance. Acquisition of EGFR-mutants is now well established and more than 50% of patients exhibit resistance in tumour cells after disease progression [26, 27]. However, it takes time to detect resistance by genetic technology because the number of resistant tumour cells must accumulate by several orders of magnitude. An optical accelerometer based on the effect of surface plasma resonance (SPR), which can detect drug molecule interactions with EGFR and distinguish EGFR molecule structural changes [28–31]. However, SPR as a probe [32] is problematic due to the limited power portion propagating in the sensing region where the analyte is located, resulting in a relatively wide resonance dip in reflectivity, a limited sensitivity and less luminescent efficiency.

Facing the above challenges, it is essential to get as much of the optical power as possible to propagate in the sensing region. Investigation of the mode power distribution suggests us to design a configuration that contains the sample in the guiding layer of the waveguide, where oscillating wave is located and most of the mode power concentrates. Addressed this issue, a hollow-core metal-cladding optofluidic resonator is developed to carry out the experiment [33]. In this design the use of double metal claddings which exhibit negative dielectric constant implies that the effective index of the guided modes can exist in the region of $0 < N < 1$, which is usually prohibited for the conventional guided modes and the surface plasmon resonance. Excitation of the ultrahigh order modes (UOMs) [34, 35] with $N \to 0$ which means group velocity approaches zero maximizes the interaction between tumor cells and the drugs. Furthermore, owing to light power concentrated in the guiding region it give rise to an enlargement of the luminescent efficiency [36]. These two measures make it possible to enhance the sensitivity of the platform. Experiment results have proved that optofluidic resonators provide an effective way to detect drug interactions in real time using EGFR and cancer cells process with CCD real-time monitoring of ATR shifts.

Biomedical Optics EXPRESS

2. Experimental system and bio-material

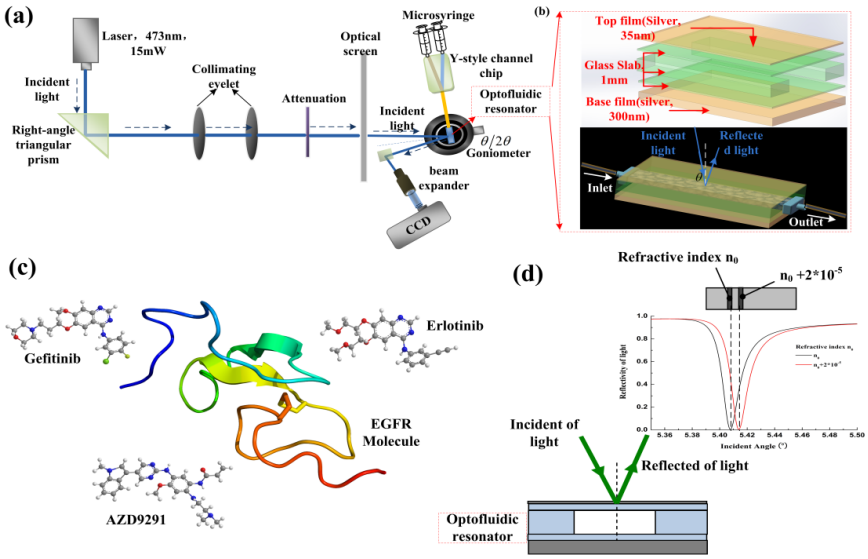

Fig. 1. Experimental system and optofluidic resonator. (a) Experimental setup. (b) optofluidic resonator; five layers from top to bottom: A 0.3-mm thick glass slide with 35 nm sliver on top, 10 × 4 mm2 rectangle channel embedded in a 0.5-mm-thick glass slab working as sample container in the guiding layer, and another 0.3-mm-thick glass coated with 300-nm-thick sliver at the bottom of the structure, the middle three layers form the guiding layer of the waveguide. These parts are optically contacted together and parallel to each other. Light is coupled into the sample channel of the fluidic resonator. (c) AZD9291, gefitinib and erlotinib drug molecular structures and NSCLC-EGFR molecular structure [37]. (d) reflectivity of light R and coupled angle θ changed, when the refraction index of the sample changed. The refractive index of the sample changed $\Delta n=2.0\times10^{-5}$ and the ATR position shifted, such that the ATR dip would shift.

The optical setup is as shown in Fig. 1(a). A computer controlled θ/2θ goniometer is applied for the accurate angular scanning of the incidence to ensure efficient energy coupling. The optofluidic resonator which acts as a symmetrical metal-cladding waveguide includes five layers. From top to the bottom, these five layers are a 35 nm silver coupling layer, a 0.3-mm glass slab, a 0.5-mm sample layer, another 0.3-mm glass slab and a 300-nm silver substrate. The size of the rectangular sample channel is 10 × 4 × 0.5 mm^3. All parts are optically contacted with excellent parallelism. The middle three layers form the guiding layer of the thickness greater than 1mm to support the sensitive ultra-high order modes (UOMs). A CCD (uEye Cockpit, EO-10012M, Resolution 1.67μm X 1.67μm) is used to record signal data, collected by close-up lenses perpendicular to the reflected light. The flow velocity is 10 μl/s, and the time interval of the recorded data is $\Delta t = 1s$. Here, the free-space coupling technique [38] is employed to excite the UOMs. After passing through a collimating system, a collimated light beam with a wavelength of 473 nm (Continuous wavelength laser, DPSS and TM00) and power of 15 mW was continuously lased incident to the cladding-metal layer of the optofluidic structure. At the synchronized angle θ, the energy of the incident light is coupled to the optofluidic resonator and a attenuated total reflection (ATR) dip is formed.

As the concentration of analyses pumped in the flow cell is changed, the ATR dip will shift due to the minute RI change. The stimulation results show that a molecular structure change in the sample, corresponding to a change of 2.0×10^{-5}. RIU (refractive index unit), will consequently result in ATR dip shift of approximately 0.014 degrees, as shown in Fig. 1(d). This means a sensitivity of 700°/RIU for the TE and TM modes. For comparison, in the reserve symmetrical waveguide sensor presented by Horvath et al. [39], the experimentally

Biomedical Optics EXPRESS

achieved sensitivities of the TM and TE modes are 33.5°/RIU and 18.8°/RIU, respectively. Figure 1(c) shows the three drugs' molecular structure and NSCLC-EGFR's molecular structure. In the experiment, NSCLC-EGFR was purchased from the Sino Biological Company using the NSCLC-EGFR protein constructed from a DNA sequence encoding the cytoplasmic domain (Met 668-Ala 1210) of human EGFR (NP_005219) fused to the N-terminal polyhistidine-tagged GST tag at the N-terminus. The recombinant human EGFR /GST chimaera consists of 780 amino acids and has a calculated molecular mass of 89.1 kDa. The molecular source is human. The protein purity was above 85% as determined by SDS-PAGE. In this experiment, the formulation was supplied as sterile 20 mM Tris, 500 mM NaCl, 10% glycerol, pH 7.4. Normally 5%-8% trehalose, mannitol and 0.01% Tween 80 are added as protectants before lyophilization. AZD9291, gefinitib and erlotinib come from the Innochem Company. Drug purity is more than 99% determined by a Spectrum Analyser. Drugs were dissolved in deionized water and all solutions were prepared immediately before use. During the analysis of cancer cell or protein interaction with drugs, in order to ensure the cells' activity, to keep constant environmental temperature at 36.8 ± 0.2°C is important. To demonstrate the human EGFR and cancer patient serum has same effect to promote the cancer cell growth and multiplication, we have a series of contrast test. And the NSCLC biopsies and serum take sampling from a terminal cancer patient at Zhengjiang Rongjun Hospital of China. The subject was a 53-year-old male whose cancer had progressed on multiple prior lines of chemotherapies and EGFR TKIs; resistance biopsy was T790M + , without evidence of the C797S mutation. The biopsies has been were separated and cell suspension in vitro.

3. Sensitive detection of drug binding sites of NSCLC-EGFR and cell by changes in the refraction index

Shown in Fig. 2, we can obtain that the NSCLC cell has been growth and multiplication in 2 and 4 culture tubes, due to 2 and 4 culture tubes has been injected same amount of patient serum and EGFR protein, respectively. And several times clear biopsies used 0.9% normal saline and were separated by dispase and 0.25% trypsin combined digestive method, and then cultured with NSCLC cells sterile culture medium. Whist the amount of 1 and 3 culture tubes cells keep the same 10 μL. According to test, we can consider the human EGFR is active and it can be considered a signification factor in promote to cancer overgrowth.

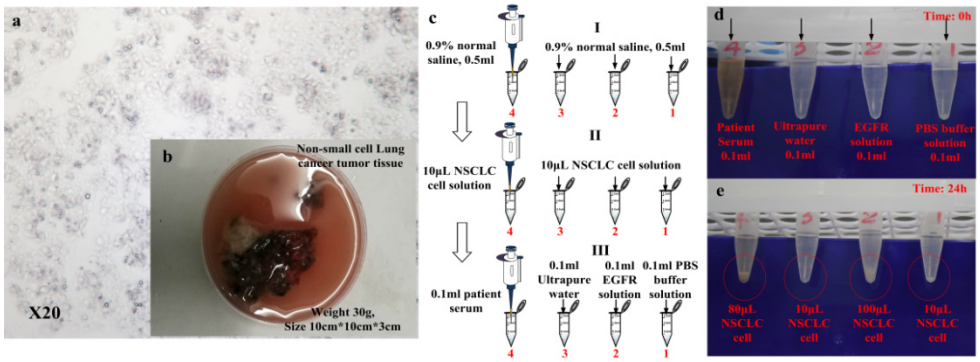

Fig. 2. EGFR protein and patient serum has same effect to promote the cancer cell growth and multiplication. (a) and (b) NSCLC biopsies from a terminal cancer patient at Zhejiang Rongjun Hospital. Small tissue samples can be obtained and examined under the microscope to confirm the diagnosis. (c) As a comparison task, to estimated the NSCLC patient serum and NSCLC EGFR protein have same effect to promote the proliferation of cancer cell. (d) At t = 0h, the picture has present that the same amount of NSCLC cell 10μL has been injected into culture tube 1-4. (e) After 24 hours, 1-4 culture tube has different cell amount. In the 4 and 2 culture tube, the amount of NSCLC cell has 80μL and 100μL, respectively. However, the amount of NSCLC cell keeps 10μL in the 1 and 3 culture tube.

Biomedical Optics EXPRESS

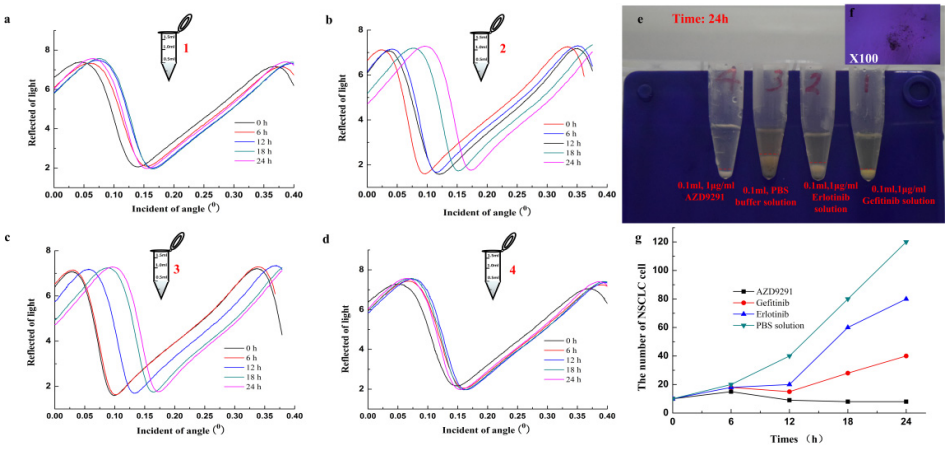

Fig. 3. Drugs, NSCLC cell, and the refraction index of the sample changed in an optofluidic resonator. (a-d) NSCLC cell has been cultured in different drug culture tube, as shown in Table 1. And we have to measure culture tube RI every 6 hours to observation of cell growth and multiplication. (e) After 24 hours, the 1-4 culture tube has different amount of NSCLC cell. (f) NSCLC cell be obtained and examined under the microscope to confirm the diagnosis from culture tube. (g) The amount of NSCLC cell has been measured every 6 hours for every culture tube.

As shown in Fig. 3, NSCLC cell has been used to verity our method. In the 4 culture tubes, we have injected into kinds of solution as shown in Table 1. In Fig. 3(g), we can observe AZD9291 inhibits NSCLC cell growth and multiplication, however, the gfitinib and erlotinib has little usefully inhibit cell growth and multiplication. And compared with EGFR protein experiment, AZD9291, gefitinib and erlotinib pesticide effect has been tested in vitro. The experimental data demonstrate that has same conclusion with EGFR.

Table 1. NSCLC cell has been cultured in different drug culture tube

The number of tubes	**1**	**2**	**3**	**4**
0.9% normal Saline	0.5ml	0.5ml	0.5ml	0.5ml
Patient serum	0.1ml	0.1ml	0.1ml	0.1ml
NSCLC Cell solution	10μL	10μL	10μL	10μL
Drugs	0.1ml, 1.0μg/ml Gefitinib solution	0.1ml, PBS buffer solution	0.1ml, 1.0μg/ml Erlotinib solution	0.1ml, 1.0μg/ml AZD9291 solution

In the experimental measurement scheme, a photodiode is employed to monitor the variation in the optical intensity of reflected light. As shown in Figs. 4(a-c), AZD9291 is injected into the resonator, and a computer-controlled θ/2θ goniometer performs angular scans, while the intensity of the reflected beam is detected by a photodiode from 0 s to 60 s. The ATR dips are recorded; the ATR dip stands at a special θ and different degree apart at times other than the beginning and ending time. This is because AZD9291 interacts with NSCLC-EGFR, RI changes and the ATR dip shifts. The ATR dip of gefitinib stands at θ and $\Delta\theta$=0.002 degrees apart from each other. The series of ATR dips of erlotinib synchronized angle differences are not especially noticeable.

Biomedical Optics EXPRESS

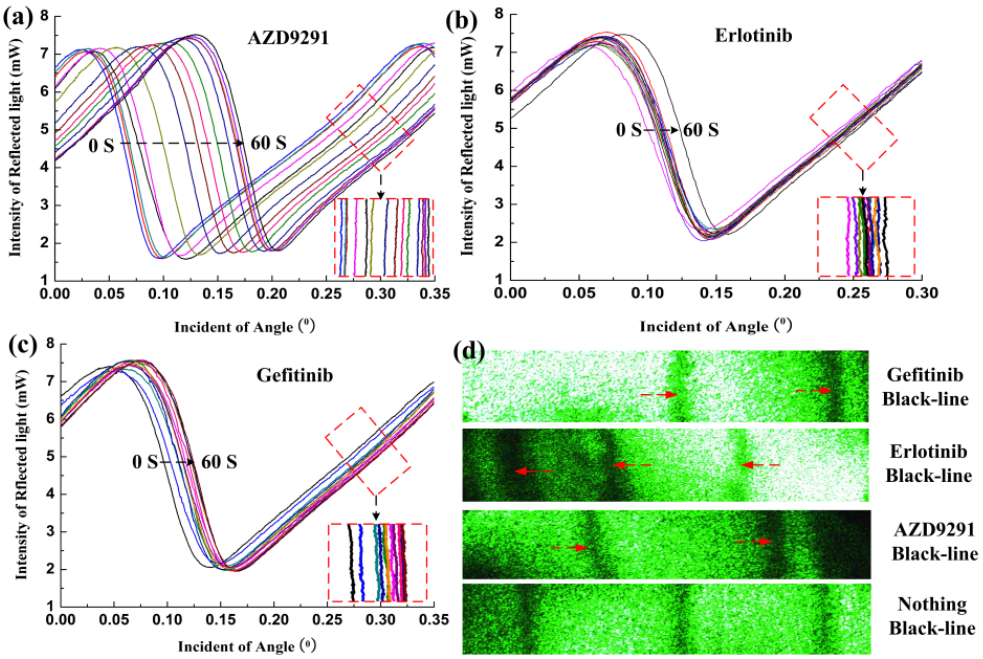

Fig. 4. Drugs, NSCLC-EGFR molecules, and the refraction index of the sample changed in an optofluidic resonator. (a-c) ATR spectrum for different times when drugs were injected into the resonator. c-d present AZD9291, erlotinib and gefitinib, respectively. (d) Different drug ATR dip images.

By comparing the gefitinib and erlotinib ATR dip synchronized angles, we can observe that the NSCLC-EGFR molecular structure significantly changed by injecting AZD9291, and the θ shifted 0.160 degrees from 0 s to 60 s. There was a θ shift of 0.037 degrees and 0.012 degrees for gefitinib and erlotinib, respectively. As the θ shift displays, we can conclude that NSCLC-EGFR molecule structure can easily be changed by the interaction with AZD9291, and the NSCLC-EGFR molecule structure is changed by the interaction with gefitinib and erlotinib to an efficiency measured by AZD9291 rate of only 37% and 12%, respectively. Including the θ shift in 60 s, we can detect the performance efficiency of AZD9291, gefitinib and erlotinib to alter NSCLC-EGFR molecule structure. Real-time monitoring of drug interactions with NSCLC-EGFR molecule times is interesting and worth studying. In the following section, we provide a key route to solve this problem using the same optofluidic resonator.

4. Real-time monitoring of the drug interaction with NSCLC-EGFR molecule by ATR dip shift

At the incident angle θ, several ATR dip are presented in the reflective pattern and captured using a CCD camera. Every 2 seconds, an ATR dip shift was captured by CCD, and the fill NSCLC-EGFR molecule solution is in a fixed position for reference. The experimental response is illustrated in Figs. 5(a-c); a 1.0 μg/ml AZD9291 solution has been injected into a resonator that can cause the number of ATR dip to change to two and ATR dip position shift. After 12 s the ATR dip shift stops, and we consider that the interaction has completed. A 1.0 g/ml gefitinib solution causes the number of ATR dip to change to two and ATR dip shift at 14 s to stop after 24 s. With an erlotinib interaction with a NSCLC-EGFR molecule, the ATR dip shift remains the same at all times and is different from AZD9291 and gefitinib, as the ATR dip shift can hardly be found, such that NSCLC-EGFR molecule structure has been little changed by erlotinib. Calculating one of the ATR dip shifts in the experimental images by

Biomedical Optics EXPRESS

MATLAB, as shown in Figs. 5(d-g), AZD9291 can cause that ATR dip shift at 2.0 μm in two seconds with a position from 53 μm to 68 μm at the reaction time.

To compare with the θ shift by the RI change in the second part, we can calculate the θ shift of 0.200 degrees by the ATR dip shift and can obtain the θ shift of 0.014 degrees of a step. That result seems to match with the 0.160 degree θ shift in the second part. There is a 0.04 degree value difference of ATR dip, we think it is mainly caused by a change in temperature of the waveguide structure due to the long time laser illumination, which makes the change in thickness and the refractive index of the materials. Due to the thickness of waveguide layer has added 1nm and the refractive index has changed 10^{-6}, and the coupling angle has shifted 0.01 degree and 0.03 degree, respectively. As we all know, the temperature enable to thickness of object d changed by thermal expansion and contraction effect. In fact, our analysis of cancer cell interaction with drugs, still keep the cells' activity by 36.8 ± 0.2 °C constant temperature environments in the processing. If the ATR peak shifts 0.04 degree, and d should added Δd~4nm or the refractive index of waveguide layer n_1 changed $\Delta n_1 \sim 13*10^{-6}$, respectively. Laser beam illuminate the waveguide structure for long time, which would enable the temperature of structure changed. Meanwhile, resulting in the thickness and refractive index of waveguide structure also changed. Therefore the ATR peak has shifted 0.04 degree that the glass layer of optofluidic resonator temperature T or refractive index changed. In addition, gefitinib can cause that ATR dip shift at 0.4 μm in two seconds with a position from 49 μm to 43 μm at the reaction time. Erlotinib can cause that ATR dip shift at 0.05 μm in two seconds with a position from 43 μm to 42 μm at a reaction time of 16 s-18 s. According to experimental data, AZD9291 can cause the NSCLC-EGFR molecule structure to change significantly in 2 seconds and react with NSCLC-EGFR molecule at the beginning and throughout the process for 12 s.

Biomedical Optics EXPRESS

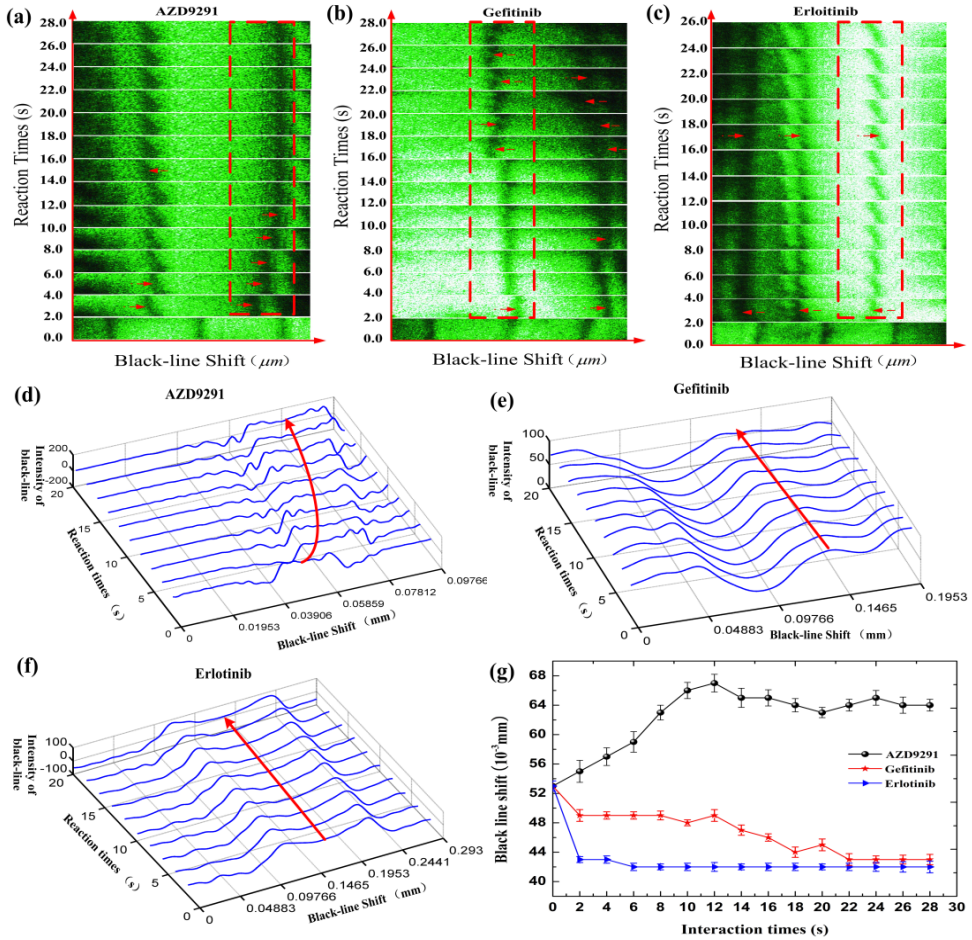

Fig. 5. Monitoring of interaction times by ATR dip shift. (a) AZD9291 interactions with NSCLC-EGFR molecules to find the interaction time from 0 s to 12 s; after 12 s the ATR dip e shift stopped. (b) Gefitinib interaction with NSCLC-EGFR molecule; ATR dip shift does not change significantly from 0 s to 14 s, but there is a significant, continuous change after 14 s and the united ATR dip shift remains stopped after 24 s. (c) Erlotinib interactions with NSCLC-EGFR molecules; the ATR dip shift maintains the same position for the entire duration. (d-f) calculation of one ATR dip shift in experimental images by MATLAB R2014a, showing AZD9291, gefitinib and erlotinib interacting with a NSCLC-EGFR molecule. (g) the ATR dip shift changed from 0 s to 24 s, including AZD9291, gefitinib and erlotinib.

In the Figs. 5(a-c), we used a red dotted line frame to label of experimental data which is plotted the curves in Figs. 5(d-f) by MATLAB R2014a. Therefore, it is clearer that the data of Figs. 5(d, e), and f come from Figs. 5(a-c). For example, after 2s time the black line move to the right and 12s the black line keep stop in the Fig. 5d, that's match with Fig. 5(a). So the line profile for Figs. 5(d-f) points to an increasing black line shift with time, and that does agree with the data presented red dotted line frame in Figs. 5(a-c). Gefitinib reaction would begin at 14 s and last 10 seconds. Erlotinib seemingly does not react at all. Therefore, the ATR dip shift can effectively and accurately monitor the processing of drugs reacting with a NSCLC-EGFR molecule in real-time. While this way can give a new method to analyse drugs when they start combining, how long the process will take and what the different combining points of the drugs are is unknown. However, we only obtain the NSCLC-EGFR molecule structure change and distinguish the drug combining sites. Providing supportive evidence that gefitinib and erlotinib have low potency against NSCLC EGFR. Quantitative analysis of

Biomedical Optics EXPRESS

AZD9291, gefitinib and erlotinib showed inhibition of the NSCLC-EGFR growth efficacy, which cannot be detected by the ATR dip shift. In the fourth part, we have accurately and quantitatively analyzed the efficacy by measuring the proportion of molecular fluorescence spot area.

5. Label-free analysis of drug efficacy by the proportion measurement of NSCLC-EGFR fluorescence spot area

The energy of incident light is coupled to the optofluidic resonator at the synchronized angles $(\theta \pm \Delta\theta,\ \Delta\theta=0.125^{\circ})$ for the black location inside the reflected spot. In the experiment, a microscopic imaging amplification system is used to make the area of the reflected light spot $S=\pi mm^2$ with ten-fold amplification $S'=10\pi mm^2$. The energy was confined in this area with an enhancement and multimode oscillating field [36]. This field can enhance protein molecule spontaneous emission to detect molecular fluorescence in the coupling area.

As shown in Figs. 6(a, b), the 0.1 mm*0.1 mm black area where light has been coupled into cavity in the excitation light beam (excitation light come from a 15 mW, λ = 405nm DPSS, TEM00 CW laser), was amplified 20-fold. There are several red and blue faculae. To observe these red and blue spot, the experimental image was transformed with a white background using MATLAB and can be seen in Fig. 5(c). When the NSCLC-EGFR molecule solution is injected into the resonator, we can detect red fluorescence and no blue fluorescence. However, blue fluorescence was detected for AZD9291, gefitinib and erlotinib. A spectrograph (Andor SR-750, 0.01nm resolution of wavelength) was used to record the signal data collected by a 0.1-mm diameter fibre-optics probe, which is near the optofluidic resonator surface, as shown in Figs. 6 (f, g) is drug and EGFR molecular fluorescent which the centre wavelength of fluorescent are 630nm and 475nm by excitation light, respectively. Using the special property of molecular fluorescence, we can achieve label-free analysis of drug efficacy using the measuring the proportion of fluorescence spot area of the NSCLC-EGFR molecule. As shown in Figs. 6 (h-j), when the excitation light knock on the chip and the centre wavelength 630nm the fluorescence of NSCLC-EGFR molecules has been excited and the fluorescence spot has been detection by CCD. When AZD9291, gefitinib and erlotinib has been injected the intensity of NSCLC-EGFR molecules has been changed in a 1 mm*1 mm area at 0 s, 5 s, 10 s and 20 s, respectivley. At 0 s, the intensity of NSCLC-EGFR molecules fluorescence which is red faculae was identical, but at 20 s, the values were significantly different. For example, red faculae almost all disappeared using AZD9291, and red fluorescence faculae remain unchanged using Erlotinib. Using gefitinib, red faculae disappeared. Thus, the proportion of NSCLC-EGFR molecule can accurately calculate AZD9291, gefitinib and erlotinib interactions to affect NSCLC-EGFR molecular efficacy, as shown in Fig. 7.

AZD9291, gefitinib and erlotinib combine with protein. After 28 s, the proportion measurement of NSCLC-EGFR fluorescence spot area differed, and we can detect the proportion as 69.60% cut by AZD9291, 40.41% cut by gefitinib and 24.15% cut by erlotinib. Compared to the numerical decrease in the three drugs, the efficiency of the NSCLC-EGFR molecule was changed by the interaction with gefitinib and erlotinib as measured by an AZD9291 rate of only 58.06% and 34.69%, respectively. In contrast, 69.60% of NSCLC-EGFR molecule inactivation required an AZD9291 drug dosage of 88.96%, and thus we can calculate an AZD9291 efficacy of 61.92% (Efficacy = Total drug dosage* Molecule Variation). The same analysis was used to calculate gefitinib efficacy as 36.82% and gefitinib efficacy as 22.25%. According to the numerical value of drug efficacy, we can accurately distinguish drug efficacy via the statistical intensity of fluorescence in the coupling area of the optofluidic resonator. Finally, a 1.000 μg/ml EGFR solution contained 0.300 μg of the EGFR molecule, and 0.300 μg EGFR inactivation required 0.484 μg of AZD9291, 0.815 μg of gefitinib and 1.348 μg of erlotinib.

Biomedical Optics EXPRESS

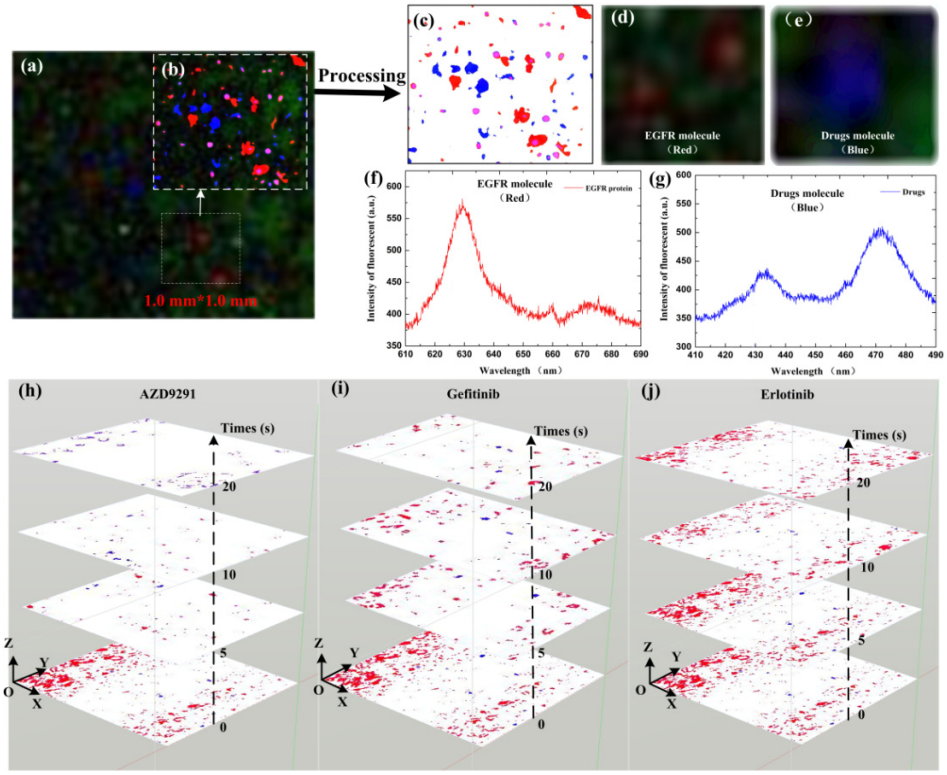

Fig. 6. Label-free analysis of efficiency by fluorescence. (a) Three ATR dip in the experimental image. In the centre, we removed a black area 1.0 mm*1.0 mm. (b) the black area was magnified twenty times using a microscopic system and red and blue faculae in the image. (c) Quantity, size and intensity of red and blue faculae remain unchanged after removing the background gradient to show the obvious fluorescence. (d,f) Red facula is the NSCLC-EGFR molecule fluorescence and spectra at before drug is injected hollow-core. (e,g) blue faculae is the drug fluorescence and spectra before NSCLC-EGFR molecule solution is injected hollow-core. (h-j) the proportion measurement of NSCLC-EGFR fluorescence spot area in a 2 mm*2 mm area at 0 s, 5 s, 10 s and 20 s.

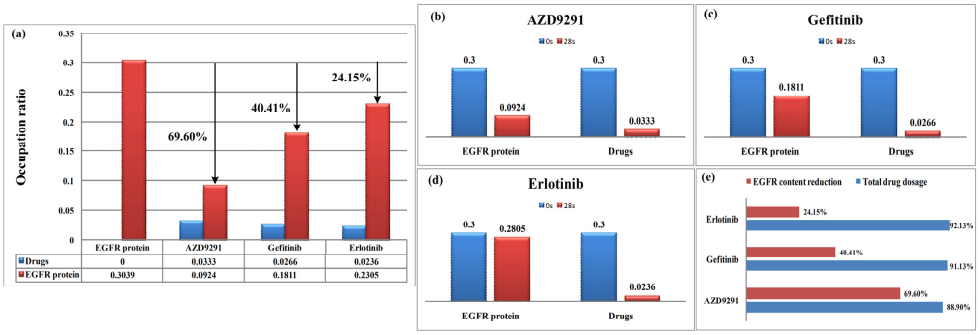

Fig. 7. Calculation and comparison of fluorescence intensity for NSCLC-EGFR molecular interaction with AZD9291, gefitinib and erlotinib. (a) We removed a black area 1 mm*1 mm and calculated the fluorescence faculae area hold proportion in the 1 mm2. When the NSCLC-EGFR molecule solution was injected into the cavity, the occupation ratio of red fluorescence faculae was 0.3039. Occupation ratios of 0.0924, 0.1811 and 0.2305 were seen for AZD9291, gefitinib and erlotinib after 28 s when injected into the cavity, respectively. The occupation ratios of blue fluorescence faculae are 0.0333, 0.0266 and 0.0236. (b-d) AZD9291, gefitinib, erlotinib and the NSCLC-EGFR molecule are the same size, and the solution concentration was 1.0 μg/ml. (e) EGFR molecule content reduction and total drug dosage.

Biomedical Optics EXPRESS

6. Conclusion

Optofluidic resonators provide an effective way to detect drug interactions in real time using EGFR and cancer cells process with CCD real-time monitoring of ATR dip shifts. Experimental results show that efficiency of gefitinib and erlotinib are only 37% and 12% of AZD9291, respectively. This work provides evidence that gefitinib and erlotinib have low potency against NSCLC EGFR and that these inhibitors can drive resistance through the acquisition of NSCLC EGFR in patient. The second method, label-free analysis of drug-EGFR binding using the molecule fluorescence intensity from the time range of 0 s to 20 s, can accurately calculate 0.300 μg of EGFR inactivation, which requires 0.484 μg of AZD9291, 0.815 μg of gefitinib and 1.348 μg of erlotinib. It is demonstrated that using the resonator we proposed can enable timely discovery of EGFR tyrosine kinase inhibitor resistance in clinical processing and accurately calculate the quantity of drugs needed to reduce and inhibit tumour growth factors in cancer patient bodies. Our current research is focused on the chemotherapy clinic research and development of anti-tumor drug with help of ATR dip shift and the fluorescence detection. Since the high power density of the resonator, enhance Raman spectroscopy may be used to distinguish the drug molecule structure. This sensitive optofluidic resonator can also be extended to measure the trace concentration of poisonous in water and monitor the air pollution in the fields of environmental protection and food safety.

Funding

National Key R&D Program of China (Grant Nos. 2017YFA0303700, 2013CBA01703); National Natural Science Foundation of China (Grant Nos. 11734011, 61235009 and 11764020).

Acknowledgments

Hailang Dai, Cheng Yin. and Zhuangqi Cao. designed and developed the concept for the optofluidic waveguide cavity at the millimetre scale, produced the hardware and software, conducted real-time, label-free and ultrasensitivity monitoring of the reaction and experiments and wrote the manuscript. Yihang Jiao and Zhangchi Sun. prepared samples during this study that were important in the development of this new research topic. Xianfeng Chen organized and supervised this work.

Disclosures

The authors declare that they have no competing financial interests.